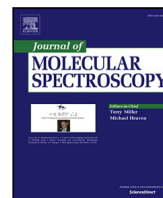




Contents lists available at ScienceDirect

Journal of Molecular Spectroscopy

journal homepage: [www.elsevier.com/locate/jmbsp](http://www.elsevier.com/locate/jmbsp)

# Calculated $^{14}\text{N}_2^{16}\text{O}$ line intensities using Radau coordinates and an accurate potential energy surface

Irina I. Mizus<sup>a</sup>, Mikhail A. Rogov<sup>b,c</sup>, Nikolai F. Zobov<sup>b</sup>, Roman I. Ovsyannikov<sup>b</sup>, Evgenii I. Lebedev<sup>b</sup>, Jonathan Tennyson<sup>d</sup>, Oleg L. Polyansky<sup>d,b,\*</sup>

<sup>a</sup> Holon Institute of Technology, Golomb Street, 52, Holon, 5810201, Israel

<sup>b</sup> Institute of Applied Physics, Russian Academy of Sciences, 46 Ulyanov Street, Nizhny Novgorod, 603950, Russia

<sup>c</sup> Department of Radiophysics, N. I. Lobachevsky State University of Nizhny Novgorod, 23 Gagarin Avenue, Nizhny Novgorod 603022, Russia

<sup>d</sup> Department of Physics and Astronomy, University College London, Gower Street, London WC1E 6BT, United Kingdom

## ARTICLE INFO

### Keywords:

Variational calculations

Nitrous oxide

Rovibrational Schrödinger equation

Line intensities

## ABSTRACT

Line intensities of the  $^{14}\text{N}_2^{16}\text{O}$  molecule are calculated using the DVR3D nuclear-motion program suite. Recently, we (Mizus *et al.*, JQSRT, **344**, 109463 (2025)) presented a potential energy surface (PES) fitted to empirical energy levels with an accuracy close to  $0.002\text{ cm}^{-1}$  and very accurate dipole moment surfaces (DMS) calculated *ab initio* using a MRCI (multi-reference configuration interactions) level of theory. However, these accurate PES and DMS did not yield uniformly accurate calculated line intensities: some transition intensities disagreed with the measured ones by orders of magnitude. Here we analyze the reasons for these inaccurately calculated line intensities and develop a spectroscopic model which gives consistently accurate intensity predictions. This improvement is based on a relative minor improvement in the accuracy of the PES, the need for which was highlighted by changing the internal coordinates used in the calculation from Jacobi to Radau. In particular, the new model predicts line intensities with close to experimental accuracy for those vibrational bands, namely  $(\nu_1\nu_2\nu_3)$  equals (5000), (4200), (3200) and (0112), whose intensities have been measured with sub-percent accuracy.

## 1. Introduction

The accuracy requirements on line intensities for metrology, climate studies, planetary physics and astrophysics can go below 0.1%. The  $\text{N}_2\text{O}$  molecule plays an important role in all these areas, as illustrated by its position among the top five molecules in the key HITRAN database [1]. However, neither experiment nor theory has yet been able to approach this level of accuracy for  $\text{N}_2\text{O}$  line intensities.

Recently, line intensities for several vibrational bands of  $^{14}\text{N}_2^{16}\text{O}$  have been measured with the sub-percent accuracy [2–5]. Two of these studies [2,3] used lasers for the intensity measurements, which increases somewhat the accuracy of the line intensity determination. Specifically, Adkins *et al.* [3] observed the (4200)←(0000) and (5000)←(0000) bands near  $1.6\text{ }\mu\text{m}$  and obtained a nominal combined standard uncertainty for the intensities of 1% for most lines (for simplicity, we use throughout the paper the vibrational state notation  $\nu_1\nu_2\nu_3$  instead of  $\nu_1\nu_2\nu_3'$ ). Odintsova *et al.* [2] studied eight  $^{14}\text{N}_2^{16}\text{O}$  transitions, mainly belonging to the (3200) and (0112) vibrational band obtaining an experimental uncertainty of about 0.4%. While Karlovets *et al.* [4] observed 47 bands belonging to the  $^{14}\text{N}_2^{16}\text{O}$ ,  $^{14}\text{N}^{15}\text{N}^{16}\text{O}$ ,  $^{15}\text{N}^{14}\text{N}^{16}\text{O}$

and  $^{14}\text{N}_2^{18}\text{O}$  isotopologues with intensities estimated to be accurate to 3% or better for most lines but up to 20% for the weakest or strongly blended lines. Subsequently, Karlovets *et al.* [5] presented measurements for a further 49 bands with the same uncertainties.

Theoretically, the  $^{14}\text{N}_2^{16}\text{O}$  molecule has been studied extensively using the effective Hamiltonian approach [6]. Variational calculations of  $^{14}\text{N}_2^{16}\text{O}$  line intensities have been made by the NASA Ames group [7] and ExoMol [8]. Recently we performed variational nuclear-motion calculation for  $^{14}\text{N}_2^{16}\text{O}$  obtaining a very accurate, fitted potential energy surface (PES) [9]. Combining wavefunctions generated using this PES with high accuracy *ab initio* dipole moment surfaces (DMS) gave very mixed results. While some vibrational bands were predicted to have intensities in line with experiment, the intensities for some bands showed large differences. For example, calculated lines of the (0112) – (0000) band measured with sub-percent accuracy by Odintsova *et al.* [2] differed by 80%; for other bands the calculated intensities were found to differ by a factor of five or more.

We address this issue in this paper which is organized as follows. Section 2 describes the calculation of new fitted PESs, which are

\* Corresponding author at: Department of Physics and Astronomy, University College London, Gower Street, London WC1E 6BT, United Kingdom.  
E-mail address: [o.polyansky@ucl.ac.uk](mailto:o.polyansky@ucl.ac.uk) (O.L. Polyansky).

<https://doi.org/10.1016/j.jms.2025.112034>

Received 22 May 2025; Received in revised form 1 July 2025; Accepted 12 July 2025

Available online 26 July 2025

0022-2852/© 2025 The Authors. Published by Elsevier Inc. This is an open access article under the CC BY license (<http://creativecommons.org/licenses/by/4.0/>).

required to give accurate wavefunctions. In Section 3 we present the  $^{14}\text{N}_2^{16}\text{O}$  intensity calculations and extensively compare these results with the experimental values, focusing on the sub-percent accurate measurements; conclusions are outlined in Section 4.

## 2. Brief review of the PES, DMS and nuclear motion program used

There are three major requirements for high accuracy *ab initio* intensity calculations: (1) an accurate program for the solution of the ro-vibrational Schrödinger equation such as DVR3D [10]; (2) an accurate potential energy surface (PES), which in practice is obtained starting from an *ab initio* PES which is then modified by fitting to experimentally-derived ro-vibrational energy levels and (3) accurate, usually purely *ab initio*, dipole moment surfaces (DMS). In this section we briefly outline the quality of all three factors used in the intensity calculations.

### 2.1. Accuracy of the molecular energy levels calculation using DVR3D program suite

Until recently the accuracy with which the vibration-rotation energy levels of a triatomic molecule could be determined by variational nuclear motion calculations using a given PES typically was found to be between 0.01 to 0.001  $\text{cm}^{-1}$ . However, huge improvements in the experimental accuracy with which the line centers can be determined [11,12] has raised the question of whether it is possible to improve spectroscopic models and hence the accuracy of the solutions of the nuclear-motion Schrödinger equation. We have shown recently [13] that for diatomics the rotation-vibration energy levels for a given potential can be determined with an accuracy of  $10^{-5} \text{ cm}^{-1}$ ; in work parallel to this study [14] we showed that for  $\text{CO}_2$ , importantly a linear molecule like  $\text{N}_2\text{O}$ , rotation-vibration energy levels can also be determined to better than  $10^{-5} \text{ cm}^{-1}$  using kinetic energy operators that are exact within the Born-Oppenheimer approximation and variational procedures. Significantly for this study, this accuracy was obtained for calculations performed in both Radau and Jacobi geometrically-defined internal coordinates. However, for  $\text{CO}_2$  convergence was found to be much faster for calculations in Radau coordinates; the desired convergence could be achieved in Radau coordinates using a final Hamiltonian matrix of dimension 2000, while in Jacobi coordinates a matrix of dimension 16 000 was needed in DVR3D. We note that normal coordinates give a very good representation of low-lying states of semi-rigid molecules such as  $\text{N}_2\text{O}$  or  $\text{CO}_2$  but become problematic for highly excited states as they can leave the true domain of the problem. Conversely, our geometrically-defined internal coordinates are rigorously defined to remain within the physical domain of the problem [15].

For the calculations presented in this paper the following DVR3D parameters have been used. Radau coordinates were used to represent the exact kinetic energy operator. For energies up to 7000  $\text{cm}^{-1}$ , Morse oscillator-like basis functions for both radial coordinates were defined using  $r_e = 2.99$ ,  $D_e = 0.3$ , and  $\omega_e = 0.01$  in atomic units; the calculations used 30, 30, and 100 discrete variable representation (DVR) grid points for the two radial and the associated Legendre functions angular coordinates, respectively, and a final vibrational Hamiltonian matrix dimension set equal to 2000; atomic masses equal to 15.994915 Da for oxygen and 14.003074 Da for nitrogen were used.

For calculations extending above 7000  $\text{cm}^{-1}$  we used expanded basis sets with new parameters as the initial basis proved to be too compact to accurately reproduce the higher energy levels. In this case Morse oscillator-like basis functions for the radial coordinates were defined using  $r_e = 2.65$ ,  $D_e = 0.03$ , and  $\omega_e = 0.0012$  in atomic units. The DVR grids were extended to 90, 90, and 100 points for two radial and the angular coordinates, respectively, and a final vibrational Hamiltonian matrix dimension was set equal to 5000.

**Table 1**

Summary of our fitted and previous PESs;  $\sigma$  gives the standard deviation of obs.-calc. for the  $N$  empirical levels [16] used in our fits.  $E_{\text{max}}$  and  $J_{\text{max}}$  are the upper limits of the energies and rotational quantum numbers,  $J$ , used when calculating the corresponding  $\sigma$  values. For our PESs the internal coordinates used in the fit are also given in parenthesis.

PES	$\sigma$ , $\text{cm}^{-1}$	$N$	$E_{\text{max}}$ , $\text{cm}^{-1}$	$J_{\text{max}}$
Schröder <i>ab initio</i> [22]	1.2520	279	7800	5
Huang et al. fitted [7]	0.038	279	7800	5
PES60hJ (Jacobi) [9]	0.0049	512	7000	15
PES96G (Jacobi) [this work]	0.0339	504	11 845	5
PES60 (Jacobi) [9]	0.0041	266	7000	5
PES60hJ (Radau) [this work]	0.0104	512	7000	15
PES96G (Radau) [this work]	0.0434	504	11 845	5
PES60f (Radau) [this work]	0.0038	266	7000	5

### 2.2. Fitted PESs and *ab initio* DMS used for the calculations

The typical accuracy of the majority of the empirically-determined energy levels is about  $10^{-3} \text{ cm}^{-1}$  [16]. This accuracy for calculated rovibrational energy levels using a variational approach has so far only been achieved for diatomic molecules. For triatomic molecules the best accuracy reached is about  $10^{-2} \text{ cm}^{-1}$  for water spectra up to 15 000  $\text{cm}^{-1}$  [17]. For triatomics comprising of heavier atoms, like ozone and carbon dioxide, the best accuracy reached until recently was about 0.03  $\text{cm}^{-1}$  [18–21]; this is approximately the accuracy of the energy levels computed by Huang et al. for  $\text{N}_2\text{O}$  [7] as part of the Ames-296K line list.

Table 1 compares standard deviations for various PESs from our previous study [9] and other published works [7,22] with respect to a set of experimentally determined energy levels of  $^{14}\text{N}_2^{16}\text{O}$  [16]; results for the PESs determined in this work are also given.

As a starting point for the intensity calculations presented here we first tested the PES60hJ potential, which was obtained by fitting, using a calculation in Jacobi coordinates, to experimental energy levels with total angular momentum  $J$  up to 15 and was shown to accurately represent high- $J$  levels [9]. However, there are known issues with using Jacobi coordinates to represent linear molecules [23]; although this issue has been successfully overcome by abandoning the standard discrete variable quadrature approximation [24], an approach has been used to successfully compute intensities in states which probe linear geometries [25], we decided to test the effect of switching coordinate systems. Switching to Radau coordinates, with the nuclear-motion problem parameters given in Section 2.1, showed that calculations performed with the PES60hJ did not precisely reproduce the previous Jacobi coordinate calculations [9]; in particular, the new calculations reproduced the 512 experimental energies up to 7000  $\text{cm}^{-1}$ , with  $J = 0, 2, 5, 10, \text{ and } 15$  with a standard deviation  $\sigma = 0.01 \text{ cm}^{-1}$  compared to 0.005  $\text{cm}^{-1}$  obtained in Jacobi coordinates. For this reason we decided to perform another fit of the potential using nuclear motion calculations in Radau coordinates and PES60hJ as the starting point.

#### 2.2.1. Fitting in Radau coordinates

In order to recover a PES with a standard deviation similar to that of PES60hJ value, we performed a new fit starting from PES60hJ and using wavefunctions computed in Radau coordinates. This fit allowed us to increase the accuracy of our predicted energy levels  $J = 0, 2$  and 5 below 7000  $\text{cm}^{-1}$  by a factor of almost four; the resulting new PES60f potential (with 60 fitted parameters) gave  $\sigma = 0.0038 \text{ cm}^{-1}$ . This and other PESs created in this work are given in the Supplementary Materials.

Table 2 presents a comparison of the experimental and calculated  $J = 0$  levels, as well as prediction of band origins ( $J = 0$  levels) between 7000 and 15 000  $\text{cm}^{-1}$ . It can be seen that the deviations from experiment for PES60f are greatly reduced compared to those given by a Radau-coordinate calculation using PES60hJ both below 7000  $\text{cm}^{-1}$  and for predictions above 7000  $\text{cm}^{-1}$ . PES60f also allowed us to obtain greatly improved predicted intensities, see Section 3 below.

### 2.2.2. Extending the PES to higher energies

In order to construct a global PES, we decided to use the energy-switching approach of Varandas [26], as we have done many times for the water molecule [27].

The final global PES96G consists of two independent parts,  $V_l$  and  $V_u$ , representing the lower and upper energy regions which are then linked by a switching function. Both  $V_l$  and  $V_u$  are new potentials, which are similar to PES96 (see Mizus et al. [9] and Table 1) in their analytic forms, but each with an independent set of 96 linear parameters optimized in the fit.  $V_l$  gives better accuracy for calculations with energies up to 7000  $\text{cm}^{-1}$ , while  $V_u$  allows us to obtain good accuracy in the energy range from 7000  $\text{cm}^{-1}$  to about 13500  $\text{cm}^{-1}$ . Each of the potentials was obtained using the fitting procedure proposed in [28,29], with the other potential fixed during the fit.

The final version of PES96G, the result of fitting both  $V_l$  and  $V_u$  potentials, was obtained using wavefunctions generated in Jacobi coordinates following the procedure described by us previously [9] for PES60hJ. A set of experimental energies up to about 12000  $\text{cm}^{-1}$ , with the values of total angular momentum quantum number  $J = 0, 2$ , and 5, as well as the set of *ab initio* points, which were used for fitting PES96G [9], were utilized to obtain two independent sets of 96 fitting parameters (see files “pot\_low.fit” and “pot\_up.fit” in Supplementary materials).

The final surfaces were stitched together smoothly using the following switching scheme analogous to the one due to Varandas [26]:

$$V_G = f_l V_l + f_u V_u, \quad (1)$$

where

$$f_{l/u} = (1 + \exp(\pm 2\alpha d_e))^{-1}, \quad (2)$$

$$\alpha = \ln\left(\frac{100}{\delta} - 1\right) / b,$$

$$d_e = V_u - E_0.$$

In the above equations the parameters  $\delta$ ,  $b$ , and  $E_0$  were obtained using trial-and-error during the fitting procedure. They have a clear meaning:  $\alpha$  is the parameter that controls the sharpness of the switching,  $E_0$  denotes the switching point,  $b$  is the width of the switching range, and  $\delta$  determines how close the switching functions,  $f_{l/u}$ , are from their asymptotic values of zero or one at the edges of the region  $E_0 \pm \frac{b}{2}$ , expressed as a percentage. After a trial-and-error adjustment procedure, these parameters were set to  $E_0 = 12850 \text{ cm}^{-1}$ ,  $b = 4000 \text{ cm}^{-1}$ , and  $\delta = 0.1$ .

The final version of our global PES96G represents 504 experimental energies used in the fitting procedure with  $\sigma = 0.034 \text{ cm}^{-1}$ . The 243 empirical levels with the energies below 7000  $\text{cm}^{-1}$ , are represented by the new potential with an unprecedented average accuracy of  $\sigma = 0.0025 \text{ cm}^{-1}$ ; the analogous accuracy for 261 levels with energies between 7000  $\text{cm}^{-1}$  and about 12000  $\text{cm}^{-1}$  is  $0.047 \text{ cm}^{-1}$ . About 20% of the 634 available empirical energies below 12000  $\text{cm}^{-1}$ , whose inclusion reduced the accuracy, were excluded from the fit.

To overcome the issue with intensity calculations in Jacobi coordinates, we switched to using Radau coordinates in DVR3D. The sparser radial DVR grids used in the calculations with a restricted energy range are too small to provide high accuracy energy levels above 7000  $\text{cm}^{-1}$ , so the larger grids were used. Switching coordinate systems, however, somewhat reduced the accuracy of the energy levels obtained using PES96G. Using Radau coordinates, calculation for PES96G reproduced 506 experimental energies with  $J = 0, 2$  and 5 with  $\sigma = 0.043 \text{ cm}^{-1}$ . 248 levels from this set, with energies below 7000  $\text{cm}^{-1}$ , are represented by the new potential with  $\sigma = 0.006 \text{ cm}^{-1}$ ; the accuracy for 256 levels with energies between 7000  $\text{cm}^{-1}$  to about 12000  $\text{cm}^{-1}$  is about  $0.06 \text{ cm}^{-1}$ .

The predicted  $J = 0$  energy levels calculated using Radau coordinates for the new PES96G are given in Table 2.

An additional comparison of the calculated levels with  $J = 1$  with empirical ones taken from the MARVEL study [16] for the three new potentials PES60hJ, PES96G, and PES60f is given in Table 1 of the Supplementary Materials. As none of these  $J = 1$  levels were used in our fits, this comparison provides an independent evaluation for the quality of our new PESes. The standard deviation for these comparisons are

$$\sigma(\text{PES60f}, < 7000 \text{ cm}^{-1}) = 0.009 \text{ cm}^{-1},$$

$$\sigma(\text{PES60hJ}, < 7000 \text{ cm}^{-1}) = 0.017 \text{ cm}^{-1},$$

$$\sigma(\text{PES96G}, < 7000 \text{ cm}^{-1}, -19.7\% \text{ outliers}) = 0.011 \text{ cm}^{-1},$$

$$\sigma(\text{PES96G}, > 7000 \text{ cm}^{-1}, -19.8\% \text{ outliers}) = 0.07 \text{ cm}^{-1}.$$

### 3. Intensity calculations

The line intensities calculated in our previous paper [9] turned out to be unexpectedly erratic. DVR3D provides very accurate solutions to the rovibrational Schrödinger equation [14], the PES used was fitted to unprecedentedly high accuracy and both DMSs used proved to be very accurate when we calculated the lines of the bands with  $v_3 = 0$  and  $l = 0$ . However, the  $v_3 = 1$  and 2 bands and the  $l = 1$  bands in many cases gave wild results, with some bands up to 4500% off. Table 3 presents the results of the calculations in Jacobi coordinates for comparison. For some bands differences with HITRAN data are absurdly high. We tested several explanations for this strange behavior. For example, we tried the option for DVR3D to avoid making the quadrature approximation [23] while evaluating integrals. As can be seen from Table 3, this did not change the results significantly.

Here we demonstrate a satisfactory solution of this problem: changing the coordinate system used for intensity calculations from Jacobi, which were used to obtain excellent fits for the  $\text{N}_2\text{O}$  PESs in the first place, to Radau coordinates. Use of wavefunctions expressed in Radau coordinates allowed very accurate line intensities to be obtained for all the bands considered in the calculations. These results are presented in the Tables 3, 4, 5 and 6; in all tables the differences between observed and calculated intensities are given as  $(\text{Obs}/\text{Calc} - 1) \times 100\%$ .

#### 3.1. Intensity calculations using Radau coordinates

An option we considered to improve the intensity predictions was changing coordinate from Jacobi to Radau in the DVR3D calculations. However, doing this meant that the  $^{14}\text{N}_2^{16}\text{O}$  energy levels calculated using the same PES were less accurate than those obtained from calculations using Jacobi coordinates in DVR3D; the problem of the erratic intensities prediction in our Jacobi coordinates remained unresolved.

However, when we refitted the PES parameters using Radau coordinates in the DVR3D we were able to both compute energy levels with a similar accuracy to the fits obtained using Jacobi coordinates and to find a solution to our problematic intensities. With these parameters we calculated the line intensities of  $^{14}\text{N}_2^{16}\text{O}$  with fully satisfactory results.

Let us first consider the results for the accurately measured intensities in the (3200) and (0112) bands [2] given in Table 4 and (4200) and (5000) bands [3] in Tables 5 and 6. As shown by Table 4, a high discrepancy of about 80% was found using Jacobi coordinates for lines in the (0112) and (3200) bands. The present Radau coordinate calculations reduced this difference to about one percent for 6 lines of these bands and to about 4% for the other two lines. We consider the agreement with experiment of our final result, given in last column, to be excellent.

The best previous calculation results are presented in the column Ames and taken from the Ames-296K line list [7]. Six lines out of eight from the column Ames of the Table 4 show discrepancies between 1.5% and 8%, and only the two remaining lines have sub-percent accuracy

Table 2

Comparison  $J = 0$  levels with the empirical ones, in  $\text{cm}^{-1}$ , for PES60hJ, PES96G, and PES60f for calculations in Radau coordinates. The empirical levels are taken from the MARVEL study [16] and the HITRAN database [1]. The levels not used for calculating the corresponding standard deviations ( $\sigma$ ) are marked by a star; for PES60hJ and PES60f the starred levels essentially represent predictions for band origins above  $7000 \text{ cm}^{-1}$ .

exp.	vib.	PES96G	exp. - PES96G	PES60hJ	exp. - PES60hJ	PES60f	exp.-PES60f
1168.1324	0 2 0 0	1168.1316	0.001	1168.1292	0.003	1168.1324	-0.000
1284.9033	1 0 0 0	1284.9056	-0.002	1284.9091	-0.006	1284.9050	-0.002
2223.7567	0 0 0 1	2223.7522	0.004	2223.7579	-0.001	2223.7587	-0.002
2322.5732	0 4 0 0	2322.5742	-0.001	2322.5706	0.003	2322.5751	-0.002
2461.9965	1 2 0 0	2461.9977	-0.001	2462.0006	-0.004	2462.0034	-0.007
2563.3403	2 0 0 0	2563.3352	0.005	2563.3419	-0.002	2563.3405	-0.000
3363.9780	0 2 0 1	3363.9753	0.003	3363.9780	0.000	3363.9822	-0.004
3466.6002	0 6 0 0	3466.5975	0.003	3466.5989	0.001	3466.5988	0.001
3480.8193	1 0 0 1	3480.8072	0.012	3480.8151	0.004	3480.8207	-0.001
3620.9430	1 4 0 0	3620.9433	-0.000	3620.9422	0.001	3620.9463	-0.003
3748.2521	2 2 0 0	3748.2527	-0.001	3748.2601	-0.008	3748.2586	-0.007
3836.3710	3 0 0 0	3836.3598	0.011	3836.3699	0.001	3836.3711	-0.000
4417.3778	0 0 0 2	4417.3602	0.018	4417.3729	0.005	4417.3745	0.003
4491.5421	0 4 0 1	4491.5369	0.005	4491.5392	0.003	4491.5438	-0.002
4630.1613	1 2 0 1	4630.1550	0.006	4630.1635	-0.002	4630.1641	-0.003
4730.8251	2 0 0 1	4730.8065	0.019	4730.8252	-0.000	4730.8284	-0.003
4767.1421	1 6 0 0	4767.1398	0.002	4767.1394	0.003	4767.1364	0.006
4910.9955	2 4 0 0	4911.0001	-0.005	4911.0045	-0.009	4911.0004	-0.005
5026.3030	3 2 0 0	5026.3035	-0.001	5026.3164	-0.013	5026.3068	-0.004
5105.6769	4 0 0 0	5105.6619	0.015	5105.6772	-0.000	5105.6773	-0.000
5529.6950	0 2 0 2	5529.6703*	0.025*	5529.6930	0.002	5529.6934	0.002
5646.7402	1 0 0 2	5646.6861*	0.054*	5646.7296	0.011	5646.7351	0.005
5762.3720	1 4 0 1	5762.3664	0.006	5762.3822	-0.010	5762.3715	0.001
5888.1059	2 2 0 1	5888.0922	0.014	5888.1259	-0.020	5888.1106	-0.005
5974.8450	3 0 0 1	5974.7868*	0.058*	5974.8512	-0.006	5974.8416	0.003
6058.6678	2 6 0 0	6058.6665	0.001	6058.6850	-0.017	6058.6704	-0.003
6192.2702	3 4 0 0	6192.2733	-0.003	6192.2922	-0.022	6192.2804	-0.010
6295.4476	4 2 0 0	6295.4424	0.005	6295.4647	-0.017	6295.4456	0.002
6373.3080	5 0 0 0	6373.2936	0.014	6373.3191	-0.011	6373.3128	-0.005
6580.8535	0 0 0 3	6580.8113*	0.042*	6580.8308	0.023	6580.8533	0.000
6768.5018	1 2 0 2	6768.4505*	0.051*	6768.5344	-0.033	6768.4962	0.005
6868.5498	2 0 0 2	6868.4237*	0.126*	6868.5748	-0.025	6868.5519	-0.002
7137.1271	3 2 0 1	7137.0947	0.033	7137.1840*	-0.057*	7137.1511*	-0.024*
7214.6797	4 0 0 1	7214.5774	0.102	7214.7411*	-0.061*	7214.6835*	-0.004*
7463.9850	4 4 0 0	7463.9524	0.033	7464.0223*	-0.037*	7464.0033*	-0.018*
7556.1361	5 2 0 0	7556.0968	0.039	7556.1560*	-0.020*	7556.1367*	-0.001*
7640.4737	6 0 0 0	7640.4431	0.031	7640.5152*	-0.042*	7640.4855*	-0.012*
7665.2728	0 2 0 3	7665.2158	0.057	7665.3376*	-0.065*	7665.3036*	-0.031*
7782.6615	1 0 0 3	7782.5196*	0.142*	7782.7226*	-0.061*	7782.6905*	-0.029*
7874.1557	1 4 0 2	7874.0984	0.057	7874.2412*	-0.086*	7874.1405*	0.015*
7998.5891	2 2 0 2	7998.5067	0.082	7998.7515*	-0.162*	7998.6176*	-0.029*
8083.9526	3 0 0 2	8083.7798*	0.173*	8084.1188*	-0.166*	8084.0434*	-0.091*
8276.3257	3 0 0 2	8276.2984	0.027	8276.5043*	-0.178*	8276.4418*	-0.116*
8376.3502	4 2 0 1	8376.2246*	0.126*	8376.5839*	-0.234*	8376.4837*	-0.134*
8452.6357	5 0 0 1	8452.5114*	0.124*	8452.8904*	-0.255*	8452.7263*	-0.090*
8714.1402	0 0 0 4	8714.0897	0.051	8714.2578*	-0.117*	8714.2449*	-0.105*
8877.0415	1 2 0 3	8876.9422	0.099	8877.3664*	-0.325*	8877.1327*	-0.091*
8976.4890	2 0 0 3	8976.2535*	0.235*	8976.9883*	-0.499*	8976.7048*	-0.216*
9108.3216	2 4 0 2	9108.2860	0.036	9108.7161*	-0.394*	9108.4572*	-0.136*
9219.0555	3 2 0 2	9218.9379*	0.118*	9219.7128*	-0.657*	9219.3962*	-0.341*
9294.9938	4 0 0 2	9294.8469*	0.147*	9295.6477*	-0.654*	9295.4103*	-0.416*
9517.8741	4 4 0 1	9517.8689	0.005	9518.4044*	-0.530*	9518.2872*	-0.413*
9606.3360	5 2 0 1	9606.2331	0.103	9607.2162*	-0.880*	9606.8245*	-0.488*
9888.5800	1 0 0 4	9888.3582*	0.222*	9889.2836*	-0.704*	9888.8626*	-0.283*
10079.5560	2 2 0 3	10 079.5057	0.050	10080.8183*	-1.262*	10080.0464*	-0.490*
10163.5927	3 0 0 3	10 163.5338	0.059	10165.3785*	-1.786*	10164.4924*	-0.900*
10429.1510	4 2 0 2	10429.2853*	-0.134*	10431.0674*	-1.916*	10430.4631*	-1.312*
10815.2510	0 0 0 5	10815.1098*	0.141*	10816.5578*	-1.307*	10815.7119*	-0.461*
10820.1280	0 4 0 4	10 820.1433	-0.015	10821.5756*	-1.448*	10820.4244*	-0.296*
11844.9700	0 2 0 5	11 844.9216	0.048	11848.4292*	-3.459*	11845.9308*	-0.961*
11964.1220	1 0 0 5	11963.6569*	0.465*	11968.6000*	-4.478*	11965.6175*	-1.495*
12891.0787	0 0 0 6	12 890.9752	0.103	12899.5539*	-8.475*	12892.5241*	-1.445*
14009.6900	1 0 0 6	14007.8996*	1.790*	14007.8454*	1.845*	14013.4874*	-3.797*
14934.2700	0 0 0 7	14933.4816*	0.788*	14928.9969*	5.273*	14937.9654*	-3.695*

in comparison with the experiment. Meanwhile, our present results (column PES60f.Radau.ai) show discrepancies of less than 2% for six out of eight lines; the two less accurately predicted line intensities from this work may be actually due to some experimental issues. Our experience suggests that lines close together in  $J$  for an isolated band should only give changes in the discrepancies as large as 3% if there are

issues with the experimental values: a similar situation occurred with the  $^{12}\text{C}^{16}\text{O}_2$  measurements from the same laboratory [19,30]. We calculated obs.-calc. values [19] for the previously-measured  $^{12}\text{C}^{16}\text{O}_2$  line intensities [31]. Some of them were accurate to about 0.3%, in line with the stated experimental uncertainties. For other lines differences of 2 to 3% were found. We suggested that these larger discrepancies were

Table 3

Differences from dipole intensities ( $I$  in cm/molecule at  $T = 296$  K scaled to 100%  $^{14}\text{N}_2^{16}\text{O}$ ) given by HITRAN [1] for strong bands. Ames denotes the Ames-296K calculation [7] and TYM the ExoMol TYM line list [8]. Our calculations used PESs designated p60 – PES60, 60hj – PES60h, 60f – PES60f, Var – PES96G, and DMS ai – our *ab initio* DMS and Sch – Schröder et al.'s DMS [22], for nuclear motion calculations performed using the given coordinates, with p60.Quad.ai denoting a Jacobi calculation without use of the quadrature approximation.

Line	$\bar{\omega}$	Band	$I$	Ames	60hj.aiRadau	60f.aiRadau	Var.aiRadau	p60.aiJacobi	p60.SchJacobi	p60.Quad.ai	TYM
R 4	4.1900	0000	8.394E-24	8.4	36.93	36.05	36.49	36.6	2.0	38.0	14.8
R 8	7.5416	0000	4.364E-23	8.1	36.38	35.53	36.38	36.2	2.1	37.8	14.5
R 4	1172.3495	0200	2.798E-21	2.8	4.79	4.01	4.40	-0.5	-0.3	0.1	-1.5
R 8	1175.7552	0200	4.566E-21	3.0	4.72	4.01	4.72	-0.5	-0.3	-0.4	-1.4
R 4	1289.0406	1000	8.313E-20	-3.3	1.88	2.00	1.88	1.0	-1.0	2.1	-0.5
R 8	1292.2870	1000	1.354E-19	-2.9	2.58	2.58	2.58	1.3	-0.8	1.8	-0.3
R 4	2326.8111	0400	2.313E-22	2.7	-11.72	-6.73	-9.65	-13.6	-13.9	-17.5	-4.5
R 8	2330.2577	0400	3.737E-22	2.3	-11.86	-7.04	-9.95	-14.1	-14.6	-18.0	-5.2
R 4	2466.1605	1200	2.677E-21	3.2	1.79	2.18	1.79	0.0	0.0	1.4	5.6
R 8	2469.4599	1200	4.354E-21	3.2	1.97	2.21	1.97	-0.2	-0.3	0.6	5.3
R 4	2567.4273	2000	1.202E-20	-0.6	0.17	-0.66	0.17	-1.3	-1.4	-0.3	0.5
R 8	2570.5747	2000	1.939E-20	-1.1	-0.05	-1.07	-0.56	-1.8	-2.1	-0.9	0.0
R 4	3625.1260	1400	3.919E-23	3.8	-4.41	-1.53	-3.71	-4.2	-5.2	-5.9	4.1
R 8	3628.4623	1400	6.354E-23	3.3	-4.88	-2.10	-4.16	-4.8	-4.9	-6.2	3.4
R 4	3752.3612	2200	3.283E-22	1.6	-2.00	-1.41	-2.29	-3.2	-3.6	-1.9	1.1
R 8	3755.5516	2200	5.333E-22	1.4	-2.33	-1.79	-2.50	-3.5	-4.0	-2.1	0.7
R 4	3840.4155	3000	7.212E-22	1.6	-0.39	-0.66	-0.80	-2.2	-2.1	-1.4	0.2
R 8	3843.4763	3000	1.162E-21	0.9	-0.68	-1.53	-1.53	-2.9	-2.9	-2.5	-0.5
R 4	4771.3396	1600	3.566E-25	-10.7	-4.91	-1.49	-4.91	-6.5	-7.1	1.2	4.5
R 8	4774.7042	1600	5.828E-25	-10.5	-4.93	-1.39	-4.78	-6.3	-7.1	-0.1	4.6
R 4	4915.1220	2400	4.273E-24	-1.0	-3.33	-0.40	-3.33	-2.5	-3.6	-3.8	1.2
R 8	4918.3457	2400	6.970E-24	-1.1	-3.33	-0.57	-3.33	-2.6	-3.8	-3.6	1.4
R 4	5030.3546	3200	2.424E-23	-0.3	-1.86	0.17	-2.26	-3.3	-4.1	-1.8	-1.4
R 8	5033.4295	3200	3.939E-23	-0.6	-2.01	-0.28	-2.50	-3.5	-4.5	-3.1	-1.6
R 4	5109.6882	4000	2.505E-23	-1.6	-2.15	-0.99	-2.91	-3.2	-3.3	-2.9	-2.7
R 8	5112.6830	4000	4.061E-23	-1.5	-2.14	-0.95	-2.61	-3.1	-3.3	-2.7	-2.5
R 4	6196.3380	3400	4.232E-25	-6.0	-6.78	-3.16	-7.19	-4.2	-4.5	-6.2	-3.8
R 8	6199.4436	3400	6.919E-25	-6.0	-6.75	-3.23	-7.13	-4.1	-4.5	-6.1	-2.7
R 4	6299.4395	4200	1.495E-24	-2.4	-2.29	1.01	-2.92	-3.6	-4.3	-1.5	-3.9
R 8	6302.3948	4200	2.434E-24	-2.4	-2.25	0.58	-3.03	-3.5	-4.3	-1.3	-3.8
R 4	6377.2978	5000	7.000E-25	-3.5	-1.27	1.45	-2.23	8.1	7.3	5.6	-2.5
R 8	6380.2504	5000	1.131E-24	-3.6	-1.65	0.98	-2.50	8.0	7.2	4.9	-2.6
R 4	592.9627	0110	5.919E-21	-6.7	-7.66	-7.52	-7.66	-8.6	-1.8	-7.7	-3.6
R 8	596.3244	0110	9.121E-21	-6.6	-7.49	-7.40	-7.49	-4.7	2.3	-4.1	0.5
R 4	1753.2724	0310	1.051E-23	6.4	1.06	2.04	2.04	26.7	8.0	28.0	26.2
R 8	1756.6582	0310	1.515E-23	6.9	1.68	1.68	1.68	14.5	-2.0	13.3	-1.4
R 4	2227.8432	0001	4.929E-19	-2.2	2.26	2.26	2.26	1.4	1.0	2.4	0.8
R 8	2230.9878	0001	8.020E-19	-1.8	2.82	2.82	2.82	1.7	0.9	3.1	1.1
R 4	2802.3854	0111	4.889E-22	1.4	1.85	1.64	1.64	-34.8	-18.4	-34.1	-34.6
R 8	2805.5426	0111	7.333E-22	1.2	1.42	1.28	1.28	-34.7	-18.3	-33.8	-34.6
R 4	3368.0939	0201	7.980E-22	-2.3	-1.12	0.00	-0.99	3.7	1.9	4.8	4.6
R 8	3371.2972	0201	1.303E-21	-2.0	-0.53	0.23	-0.53	3.8	1.9	4.3	4.7
R 4	3484.8524	1001	1.626E-20	-5.0	-4.35	-3.79	-4.35	-5.4	-5.2	-4.5	-6.5
R 8	3487.8906	1001	2.636E-20	-5.0	-4.15	-3.44	-4.15	-5.4	-5.4	-4.4	-6.5
R 4	3935.3551	0311	2.880E-25	--	-1.37	0.35	-1.37	2.1	-25.4	-26.2	5.8
R 4	4066.0208	1111	6.232E-24	1.3	-1.08	-0.13	-0.92	53.1	12.8	54.9	46.4
R 8	4069.0748	1111	8.960E-24	0.9	-1.54	-0.67	-1.43	39.5	3.4	41.8	33.5
R 4	4421.3604	0002	5.828E-22	33.8	7.93	5.77	7.33	4.1	6.1	5.7	26.2
R 8	4424.2974	0002	9.404E-22	33.7	7.72	5.78	7.23	2.8	4.7	4.4	24.5
R 4	4495.6812	0401	9.535E-25	--	3.64	2.42	1.87	8.3	27.7	41.0	25.0
R 8	4498.9298	0401	1.566E-24	--	3.03	1.69	1.69	9.0	28.6	41.5	25.0
R 4	4634.2236	1201	5.091E-23	-9.0	-2.47	0.02	-2.28	-1.2	-5.4	0.5	-7.4
R 8	4637.3198	1201	8.273E-23	-9.4	-2.90	-0.33	-2.78	-1.3	-5.6	0.3	-7.5
R 4	4734.8083	2001	3.606E-22	-4.0	-0.39	1.86	-0.11	-0.7	-1.0	0.0	-5.3
R 8	4737.7465	2001	5.869E-22	-3.7	-0.19	2.25	0.15	-0.3	-0.7	0.4	-4.9
R 4	4981.6881	0112	2.232E-24	2.5	-2.96	-3.79	-2.96	-90.0	-74.0	-89.9	-88.7
R 8	4984.6404	0112	3.333E-24	2.4	-3.11	-3.95	-3.11	-90.1	-74.2	-90.2	-88.7
R 4	5533.7095	0202	4.273E-25	30.6	23.50	23.14	22.09	675.6	492.8	492.2	454.5
R 8	5536.7099	0202	6.970E-25	31.0	23.80	23.58	22.50	652.6	477.7	476.5	437.8
R 4	5650.6691	1002	8.556E-24	57.1	7.76	8.30	7.08	-16.4	4.5	-13.1	66.5
R 8	5653.4986	1002	1.374E-23	56.3	7.34	7.34	6.51	-18.0	-2.1	-14.9	62.6
R 4	5892.1134	2201	3.242E-24	-12.7	-7.64	-4.37	-7.37	-11.9	-17.1	-9.0	-16.8
R 8	5895.0997	2201	5.293E-24	-12.7	-7.63	-4.29	-7.30	-11.6	-16.8	-8.5	-16.4
R 4	5978.7849	3001	8.798E-24	-9.0	-2.46	0.89	-2.14	8.5	1.0	7.2	-11.0
R 8	5981.6365	3001	1.434E-23	-8.5	-1.78	0.99	-1.78	9.2	1.7	8.3	-10.4
R 4	6584.7324	0003	1.182E-23	25.7	12.57	13.65	12.57	67.8	3.0	65.4	-21.4
R 8	6587.4616	0003	1.909E-23	25.7	12.29	13.63	12.29	65.1	1.8	64.5	-22.3
R 4	6872.4284	2002	3.091E-25	-18.4	13.22	11.19	15.77	4561.5	104.7	-95.7	-52.6
R 8	6875.1572	2002	5.010E-25	-18.3	13.35	11.09	15.70	4545.3	106.1	-94.3	-52.6
R 4	7141.0757	3201	3.545E-25	-10.2	-6.96	-3.67	-6.22	-10.9	-24.2	-6.3	-20.3
R 8	7143.9444	3201	5.747E-25	-10.7	-7.46	-4.06	-6.70	-11.2	-24.5	-6.4	-20.6
R 4	7218.5881	4001	3.384E-25	-16.7	-11.41	-8.54	-10.71	103.3	50.9	80.5	-24.1
R 8	7221.3766	4001	5.495E-25	-16.5	-11.08	-8.26	-10.36	103.8	51.5	81.4	-23.9

**Table 4**

Comparison with the intensity measurements of Odintsova et al. [2] in cm/molecule at  $T = 296$  K. Ames gives the obs.-calc. values for the Ames-296K line list [7], p60.ai represents our calculations with the PES60 and our *ab initio* DMS [9] while p60.Sch calculations used PES60 and the DMS due to Schroder et al. [22]; in both cases Jacobi coordinates were used in the DVR3D calculations. The next three columns used Radau coordinates with our *ab initio* DMS [9] and three different PESs: PES60hJ, PES96G and PES60f. The final column, designated PES60f.Radau.ai, gives the final result of this work.

line	$\tilde{\omega}$ cm <sup>-1</sup>	Band	Obs.	Ames	p60.ai	p60.Sch.	PES60hJ.Radau.ai	PES96G.Radau.ai	PES60f.Radau.ai
P41	4984.29	(3200)	6.23E-24	-2.5			-5.61	-5.89	-3.86
R7	4983.92	(0112)	3.19E-24	7.6	-89.6	-73.2	-0.31	-0.31	-1.24
P43	4983.76	(3310)-(0110)	2.67E-25	-0.3			-2.91	-3.26	-1.11
R6	4983.19	(0112)	2.83E-24	4.3	-89.9	-73.9	-3.41	-3.41	-4.07
P42	4983.06	(3200)	5.55E-24	0.3			-2.80	-3.31	-1.07
P43	4981.83	(3200)	4.84E-24	1.5			-1.63	-2.02	0.21
R4	4981.69	(0112)	2.28E-24	6.8	-89.6	-73.2	-0.87	-0.87	-1.72
P44	4980.58	(3200)	4.21E-24	2.9			-0.24	-0.71	1.45

**Table 5**

Differences between measured intensities for the (4200) band ( $I$  in cm/molecule at  $T = 296$  for 100% <sup>14</sup>N<sub>2</sub><sup>16</sup>O) due to Adkins et al. [3] and calculations: Ames - Ames-296K line list [7], PES60hJ.R.ai/PES60f.R.ai/PES96G.R.ai - PES60hJ/PES60f/PES96G obtained in Radau coordinates and our *ab initio* DMS, TYM - Exomol TYM list [8].

Line	$\tilde{\omega}$ /cm <sup>-1</sup>	$I$	Ames	PES60hJ.R.ai	PES96G.R.ai	PES60f.R.ai	TYM
P17e	6279.406202	2.80E-24	-1.4			0.72	
P16e	6280.455528	2.84E-24	-1.0			1.43	
P15e	6281.491611	2.86E-24	-0.2			1.78	
P14e	6282.514458	2.80E-24	-1.6			0.36	
P13e	6283.524079	2.76E-24	-1.2			0.73	
P12e	6284.52048	2.80E-24	0.2			4.87	
P11e	6285.503667	2.56E-24	-2.5			-0.39	
P10e	6286.473645	2.46E-24	-2.3	-2.38	-3.15	0.82	-4.1
P9e	6287.430421	2.29E-24	-3.1	-2.97	-3.78	0.00	-4.8
P8e	6288.373997	2.18E-24	0.0	0.00	-0.91	3.32	-1.7
P7e	6289.304378	1.92E-24	-2.6	-2.54	-3.52	0.52	-4.3
P6e	6290.221565	1.69E-24	-2.8	-2.87	-3.43	0.00	-4.5
P5e	6291.125559	1.45E-24	-2.4	-2.68	-3.33	0.69	-4.1
P4e	6292.016361	1.19E-24	-2.0	-1.65	-2.46	0.85	-3.7
P3e	6292.893972	9.06E-25	-2.2	-2.27	-2.89	0.89	-3.8
P2e	6293.758388	6.03E-25	-3.6	-3.67	-4.29	-0.50	-5.2
P1e	6294.609609	2.99E-25	-5.3	-5.38	-5.97	-2.29	-6.7
R0e	6296.272448	3.07E-25	-3.3	-3.46	-4.06	-0.32	-4.7
R1e	6297.084057	6.22E-25	-1.8	-1.74	-2.51	1.30	-3.3
R2e	6297.882451	9.23E-25	-2.1	-2.22	-2.84	0.98	-3.6
R3e	6298.667624	1.21E-24	-2.7	-2.42	-3.2	0.00	-4.2
R4e	6299.439566	1.50E-24	-2.0	-1.96	-2.92	1.35	-3.6
R5e	6300.198270	1.75E-24	-2.9	-2.78	-3.85	0.00	-4.4
R6e	6300.943725	2.03E-24	-1.2	-1.46	-1.93	2.01	-2.7
R7e	6301.675921	2.23E-24	-2.4	-2.62	-3.04	0.45	-3.9
R8e	6302.394846	2.24E-24	-10.1	-10.04	-10.76	-7.44	-11.5
R9e	6303.100487	2.62E-24	-2.0	-2.24	-2.60	1.16	-3.5
R10e	6303.792831	2.76E-24	-1.3			0.73	
R11e	6304.471864	2.89E-24	-1.4			1.05	
R12e	6305.137572	2.98E-24	-1.5			0.68	
R13e	6305.789939	3.07E-24	-0.9			1.32	
R14e	6306.428948	3.10E-24	-1.0			0.98	
R15e	6307.054582	3.11E-24	-1.5			0.65	
R16e	6307.666825	3.11E-24	-1.1			0.97	

caused by experimental problems, which was borne out by subsequent re-measurement of the intensities [30].

Tables 5 and 6 compare calculations of the (4200) and (5000) bands with sub-percent accuracy measurements [3]. For the (4220) band the calculations taken from the Ames-296K line list and our Jacobi coordinate calculations [9] give discrepancies of about 3%. Calculations in Radau coordinates show much higher accuracy, which is close to the experimental uncertainty. In particular, 29 out of 34 lines presented for  $J \leq 17$  are predicted with either of sub-percent or one percent accuracy. Only 5 lines show discrepancies between 2 and 7.5%. For these 5 lines the arguments presented above are valid: we would encourage re-measurement of the intensities of these 5 lines. We are confident this would confirm the sub-percent accuracy of our calculations.

### 3.1.1. Comparisons with HITRAN

To estimate the accuracy of the intensity calculations using the various PESs plus our *ab initio* DMS [9] and that from the Schröder

et al. [22], we calculated intensities for the R4 and R8 lines of the many bands presented in the HITRAN database [1]; the HITRAN database data is mostly based on somewhat less accurate intensity measurements than those considered above. The results of these comparisons are given in Table 3 where the differences are again represented as  $(\text{Obs}/\text{Calc} - 1) \cdot 100, \%$ . Table 3 also presents corresponding line intensities taken from Ames-296K line list [7] for comparison.

An important result is that swapping the coordinate system used to compute the wavefunctions from Jacobi coordinates, used in all calculations of our previous paper [9], to Radau coordinate system, completely solves the problem of large discrepancies found previously for some bands when using Jacobi coordinates calculations. All the bands presented in Table 3 calculated in Radau coordinates give very reasonable discrepancies, comparable or better than the error code given for them by HITRAN. All the ridiculous discrepancies have disappeared in these calculations. The worst discrepancies are 23% for the (0202) band and 36% for the (0000) band. Only two other bands are more than 10% off the values presented in HITRAN. 22 out of 37 bands

**Table 6**

Differences between measured intensities for the (5000) band ( $I$  in cm/molecule at  $T = 296$  for 100%  $^{14}\text{N}_2^{16}\text{O}$ ) due to Adkins et al. [3] and calculations. Ames – Ames-296K line list [7], PES60hJ.R.ai/PES60f.R.ai/PES96G.R.ai – PES60hJ/PES60f/PES96G obtained in Radau coordinates and our *ab initio* DMS, Ames.ai – Ames-296K PES and our *ab initio* DMS, Ames.Sch – Ames-296K and DMS by Schröder et al. , TYM – ExoMol TYM line list [8].

Line	$\tilde{\omega}/\text{cm}^{-1}$	$I$	Ames	PES60hJ.R.ai	PES96G.R.ai	PES60f.R.ai	Ames.ai	Ames.Sch	TYM
P17e	6357.260952	1.271E-24	-3.1			0.87			
P16e	6358.309647	1.274E-24	-4.0			0.31			
P15e	6359.345443	1.290E-24	-3.2			0.78			
P14e	6360.368289	1.282E-24	-3.4			0.94			
P13e	6361.378139	1.272E-24	-2.8			0.95			
P12e	6362.374947	1.234E-24	-3.3			0.33			
P11e	6363.358674	1.186E-24	-3.8			0.51			
P10e	6364.329281	1.130E-24	-4.7	-2.59	-3.42	0.00	10.4	8.1	-3.6
P9e	6365.286733	1.080E-24	-3.2	-0.92	-1.82	1.89	12.2	9.8	-2.0
P8e	6366.231001	1.087E-24	5.5	7.62	6.57	10.92	22.2	19.6	6.7
P7e	6367.162054	8.929E-25	-4.3	-2.09	-3.05	0.55	10.8	8.5	-3.2
P6e	6368.079869	7.778E-25	-5.7	-3.50	-4.45	-0.79	9.2	6.9	-4.6
P5e	6368.984422	6.707E-25	-4.9	-2.66	-3.64	-0.04	10.0	7.8	-3.9
P4e	6369.875696	5.485E-25	-4.9	-2.75	-3.60	-0.09	10.0	7.8	-3.9
P3e	6370.753673	4.111E-25	-6.6	-3.40	-5.28	-1.89	8.0	5.8	-5.6
P2e	6371.618341	2.859E-25	-3.9	-1.75	-2.76	1.02	11.1	8.9	-2.9
P1e	6372.469689	1.434E-25	-4.5	-2.45	-3.11	0.28	10.4	8.3	-3.4
R0e	6374.132400	1.394E-25	-7.7	-5.81	-6.44	-3.19	10.3	4.6	-6.7
R1e	6374.943758	2.939E-25	-2.3	-0.03	-1.04	2.76	10.3	10.7	-1.3
R2e	6375.741786	4.242E-25	-5.3	-3.15	-4.03	-0.42	9.4	7.4	-4.3
R3e	6376.526487	5.586E-25	-5.3	-3.19	-4.02	-0.43	9.3	7.3	-4.3
R4e	6377.297871	6.838E-25	-5.8	-3.55	-2.23	-0.90	7.3	6.8	-4.8
R5e	6378.055947	8.121E-25	-4.8	-2.63	-3.55	0.14	9.8	7.9	-3.8
R6e	6378.800729	9.202E-25	-5.2	-3.03	-3.95	-0.41	9.3	7.4	-4.3
R7e	6379.532233	1.077E-24	-0.1	2.57	1.60	4.56	15.2	13.2	0.9
R8e	6380.250481	1.125E-24	-4.1	-2.17	-3.02	0.45	10.6	8.7	-3.1
R9e	6380.955494	1.202E-24	-4.3	-2.28	-3.06	0.01	10.4	8.4	-3.3
R10e	6381.647299	1.264E-24	-3.7			0.32			
R11e	6382.325924	1.307E-24	-4.4			-0.23			
R12e	6382.991403	1.356E-24	-3.7			0.44			
R13e	6383.643771	1.380E-24	-3.9			0.00			
R14e	6384.283066	1.417E-24	-2.3			1.94			
R15e	6384.909332	1.441E-24	-0.8			2.93			
R16e	6385.522614	1.387E-24	-3.9			-0.22			

are only about 1 to 2% off their HITRAN values. Altogether this is an excellent result: for nearly half the bands our predictions are between 2 and 10 times more accurate than those of the Ames-296K line list [7].

There is one more interesting result which follows from the Tables 3–6. Previously [17] we found that improving the PES for the water molecule so that the standard deviation with which we predicted energy levels dropped from about 0.025 to 0.013  $\text{cm}^{-1}$  resulted in a change of the line intensities by up to 2 percent for about 20% of the bands; while the majority of the line intensities were unchanged within 0.1%. A very different situation can be seen in Tables 3 to 6. A small change in the standard deviation of the PES of  $^{14}\text{N}_2^{16}\text{O}$  from  $\sigma = 0.006$  to 0.004  $\text{cm}^{-1}$  results in a change of more than 1% in the line intensities for very many band lines. In Table 4 the column PES96G.Radau.ai corresponds to the calculations with PES, fitted to experimental levels in Jacobi coordinates, which gives  $\sigma = 0.006 \text{ cm}^{-1}$  in Radau coordinates, and the column PES60f.Radau.ai represents the results with the PES fitted in Radau coordinates with  $\sigma < 0.004 \text{ cm}^{-1}$ . The same behavior can also be seen in Tables 3, 5 and 6.

The conclusion from this finding is that even a seemingly insignificant change of the PES can result in a serious change of the intensity even for an isolated band. This finding needs to be borne in mind in the quest of generating sub-percent or even sub-per-mille calculated line intensities for the molecules important for atmospheric studies. Even more important is the role this might play in metrology where attempts to achieve line intensity accurate to  $10^{-2}$  or even  $10^{-3}$  % for measurement of temperature, pressure and isotopic substitution [32, 33].

#### 4. Conclusion

In this paper we resolve the problem of inaccurately calculated  $^{14}\text{N}_2^{16}\text{O}$  intensities for lines involving excitation of  $\nu_3$  and/or  $l$  identified by us previously [9] for calculations performed using Jacobi

coordinates. Our solution is to change the coordinate system used to calculate the wavefunctions to Radau coordinates. Excellent reproduction of the experimental line intensities is achieved, superseding those presented in line lists such as Ames-296K [7], and ExoMol TYM [8], as well as our previous study [9]. In particular, four bands intensities, presented in Tables 4, 5, and 6 and measured with the sub-percent accuracy in [3] and [2] are reproduced within the experimental error. The previous variational calculations of these accurately measured bands gave the accuracy about 3 to 5 percent.

We also solve the problem of extremely large deviations of the line intensities of some bands which turned out to be due to the use of Jacobi coordinates. The reason why the Jacobi coordinates could not be used for the intensity calculations of  $^{14}\text{N}_2^{16}\text{O}$  still remains unclear. Practically all the bands presented in HITRAN are reproduced in our calculations more accurately than in the variational calculations given in the literature [7–9].

The solution of the intensity problem combined with the near experimental accuracy achieved for calculated line centers [9] facilitates the computation of a highly accurate line list for  $^{14}\text{N}_2^{16}\text{O}$ .

#### CRedit authorship contribution statement

**Irina I. Mizus:** Writing – review & editing, Investigation, Formal analysis, Data curation. **Mikhail A. Rogov:** Investigation. **Nikolai F. Zobov:** Writing – review & editing, Investigation. **Roman I. Ovsyannikov:** Methodology, Investigation, Formal analysis. **Evgenii I. Lebedev:** Investigation. **Jonathan Tennyson:** Writing – review & editing, Formal analysis. **Oleg L. Polyansky:** Writing – original draft, Methodology, Formal analysis, Conceptualization.

#### Declaration of competing interest

The authors declare no conflict of interest.

## Acknowledgments

We acknowledge support by State Project IAP RAS No. FFUF-2024-0016. This work was funded by ERC Advanced Investigator Project 883830.

## Appendix A. Supplementary data

The supplementary material contains (A) the potential energy surfaces created in this work; (B) full results of the fits in terms of observed minus calculated comparisons.

Supplementary material related to this article can be found online at <https://doi.org/10.1016/j.jms.2025.112034>.

## Data availability

The data is all supplied as supplementary material.

## References

- I.E. Gordon, L.S. Rothman, R.J. Hargreaves, R. Hashemi, E.V. Karlovets, F.M. Skinner, E.K. Conway, C. Hill, R.V. Kochanov, Y. Tan, P. Wcisło, A.A. Finenko, K. Nelson, P.F. Bernath, M. Birk, V. Boudon, A. Campargue, K.V. Chance, A. Coustenis, B.J. Drouin, J. Flaud, R.R. Gamache, J.T. Hodges, D. Jacquemart, E.J. Mlawer, A.V. Nikitin, V.I. Perevalov, M. Rotger, J. Tennyson, G.C. Toon, H. Tran, V.G. Tyuterev, E.M. Adkins, A. Baker, A. Barbe, E. Canè, A.G. Császár, A. Dudaryonok, O. Egorov, A.J. Fleisher, H. Fleurbaey, A. Foltynowicz, T. Furtenbacher, J.J. Harrison, J. Hartmann, V. Horneman, X. Huang, T. Karman, J. Karns, S. Kass, I. Kleiner, V. Kofman, F. Kwabia-Tchana, N.N. Lavrentieva, T.J. Lee, D.A. Long, A.A. Lukashchinskaya, O.M. Lyulin, V.Y. Makhnev, W. Matt, S.T. Massie, M. Melosso, S.N. Mikhailenko, D. Mondelain, H.S.P. Müller, O.V. Naumenko, A. Perrin, O.L. Polyansky, E. Raddaoui, P.L. Raston, Z.D. Reed, M. Rey, C. Richard, R. Tóbiás, I. Sadiek, D.W. Schwenke, E. Starikova, K. Sung, F. Tamassia, S.A. Tashkun, J. Vander Auwera, I.A. Vasilenko, A.A. Vigin, G.L. Villanueva, B. Vispoel, G. Wagner, A. Yachmenev, S.N. Yurchenko, The HITRAN molecular spectroscopic database, *J. Quant. Spectrosc. Radiat. Transfer* 277 (2022) 107949, <http://dx.doi.org/10.1016/j.jqsrt.2021.107949>.
- T.A. Odintsova, E. Fasci, S. Gravina, L. Gianfrani, A. Castrillo, Optical feedback laser absorption spectroscopy of N<sub>2</sub>O at 2 μm, *J. Quant. Spectrosc. Radiat. Transfer* 254 (2020) 107190, <http://dx.doi.org/10.1016/j.jqsrt.2020.107190>.
- E.M. Adkins, D.A. Long, A.J. Fleisher, J.T. Hodges, Near-infrared cavity ring-down spectroscopy measurements of nitrous oxide in the (4200)–(0000) and (5000)–(0000) bands, *J. Quant. Spectrosc. Radiat. Transfer* 262 (2021) 107527, <http://dx.doi.org/10.1016/j.jqsrt.2021.107527>.
- E. Karlovets, S. Kass, S. Tashkun, A. Campargue, The absorption spectrum of nitrous oxide between 8325 and 8622 cm<sup>-1</sup>, *J. Quant. Spectrosc. Radiat. Transfer* 262 (2021) 107508, <http://dx.doi.org/10.1016/j.jqsrt.2021.107508>.
- E. Karlovets, S. Kass, S. Tashkun, A. Campargue, The absorption spectrum of nitrous oxide between 7647 and 7918 cm<sup>-1</sup>, *J. Quant. Spectrosc. Radiat. Transfer* 288 (2022) 108199, <http://dx.doi.org/10.1016/j.jqsrt.2022.108199>.
- S.A. Tashkun, V.I. Perevalov, N.N. Lavrentieva, Nod-1000, the high-temperature nitrous oxide spectroscopic databank, *J. Quant. Spectrosc. Radiat. Transfer* 177 (2016) 43–48, <http://dx.doi.org/10.1016/j.jqsrt.2015.11.014>.
- X. Huang, D.W. Schwenke, T.J. Lee, Highly accurate potential energy surface and dipole moment surface for nitrous oxide and 296 K infrared line list for <sup>14</sup>N<sub>2</sub>O and minor isotopologues, *Mol. Phys.* 122 (2024) e2232892, <http://dx.doi.org/10.1080/00268976.2023.2232892>.
- S.N. Yurchenko, T. Mellor, J. Tennyson, Exomol line lists LIX. high-temperature line list for N<sub>2</sub>O, *Mon. Not. R. Astron. Soc.* 534 (2024) 1364–1375, <http://dx.doi.org/10.1093/mnras/stae2201>.
- I.I. Mizus, N.F. Zobov, V.Y. Makhnev, R.I. Ovsyannikov, M.A. Rogov, J. Tennyson, O.L. Polyansky, Approaching experimental accuracy for triatomic spectra using variational calculations: Potential energy and dipole moment surfaces of N<sub>2</sub>O, *J. Quant. Spectrosc. Radiat. Transfer* 344 (2025) 109463, <http://dx.doi.org/10.1016/j.jqsrt.2025.109463>.
- J. Tennyson, M.A. Kostin, P. Barletta, G.J. Harris, O.L. Polyansky, J. Ramanlal, N.F. Zobov, DVR3D: a program suite for the calculation of rotation-vibration spectra of triatomic molecules, *Comput. Phys. Comm.* 163 (2004) 85–116.
- J. Wang, Y.R. Sun, L.G. Tao, A.W. Liu, S.M. Hu, Communication: Molecular near-infrared transitions determined with sub-kHz accuracy, *J. Chem. Phys.* 147 (2017) 091103, <http://dx.doi.org/10.1063/1.4998763>.
- J. Wang, C.-L. Hu, A.-W. Liu, Y. Sun, Y. Tan, S.-M. Hu, Saturated absorption spectroscopy near 1.57 μm and revised rotational line list of <sup>12</sup>C<sup>16</sup>O, *J. Quant. Spectrosc. Radiat. Transfer* 270 (2021) 107717, <http://dx.doi.org/10.1016/j.jqsrt.2021.107717>.
- I.I. Mizus, L. Lodi, J. Tennyson, N.F. Zobov, O.L. Polyansky, An analysis of the accuracy of line intensities calculations using DUO and LEVEL program package, *J. Mol. Spectrosc.* 368 (2022) 111621, <http://dx.doi.org/10.1016/j.jms.2022.111621>.
- R.I. Ovsyannikov, I.I. Mizus, A.N. Perri, J. Tennyson, S.N. Yurchenko, A. Mitrushchenkov, N.F. Zobov, M.A. Rogov, O.L. Polyansky, High accuracy solution of the rovibrational Schrödinger equation for triatomic molecules, 2025, submitted for publication.
- B.T. Sutcliffe, J. Tennyson, A general treatment of vibration-rotation coordinates for triatomic molecules, *Intern. J. Quantum Chem.* 39 (1991) 183–196.
- J. Tennyson, T. Furtenbacher, S.N. Yurchenko, A.G. Császár, Empirical rovibrational energy levels for nitrous oxide, *J. Quant. Spectrosc. Radiat. Transfer* 316 (2024) 108902, <http://dx.doi.org/10.1016/j.jqsrt.2024.108902>.
- I.I. Mizus, A.A. Kyuberis, N.F. Zobov, V.Y. Makhnev, O.L. Polyansky, J. Tennyson, High accuracy water potential energy surface for the calculation of infrared spectra, *Phil. Trans. R. Soc. Lond. A* 376 (2018) 20170149, <http://dx.doi.org/10.1098/rsta.2017.0149>.
- D. Jacquemart, V.Y. Makhnev, N.F. Zobov, J. Tennyson, O.L. Polyansky, Synthesis of *ab initio* and effective Hamiltonian line lists for, *J. Quant. Spectrosc. Radiat. Transfer* 269 (2021) 107651, <http://dx.doi.org/10.1016/j.jqsrt.2021.107651>.
- O.L. Polyansky, K. Bielska, M. Ghysels, L. Lodi, N.F. Zobov, J.T. Hodges, J. Tennyson, High accuracy CO<sub>2</sub> line intensities determined from theory and experiment, *Phys. Rev. Lett.* 114 (2015) 243001, <http://dx.doi.org/10.1103/PhysRevLett.114.243001>.
- V.G. Tyuterev, R.V. Kochanov, S.A. Tashkun, F. Holka, P.G. Szalay, New analytical model for the ozone electronic ground state potential surface and accurate *ab initio* vibrational predictions at high energy range, *J. Chem. Phys.* 139 (2013) 134307, <http://dx.doi.org/10.1063/1.4821638>.
- X. Huang, D.W. Schwenke, R.S. Freedman, T.J. Lee, CO<sub>2</sub> dipole moment surface and IR line lists: Toward 0.1 % uncertainty for CO<sub>2</sub> IR intensities, *J. Phys. Chem. A* 126 (2022) 5940–5964, <http://dx.doi.org/10.1021/acs.jpca.2c01291>.
- B. Schröder, P. Sebald, C. Stein, O. Weser, P. Botschwina, Challenging high-level *ab initio* rovibrational spectroscopy: The nitrous oxide molecule, *Z. Phys. Chem.* (2015) <http://dx.doi.org/10.1515/zpch-2015-0622>.
- J.R. Henderson, J. Tennyson, B.T. Sutcliffe, All the bound vibrational states of H<sub>3</sub><sup>+</sup>: a reappraisal, *J. Chem. Phys.* 98 (1993) 7191–7203.
- J. Tennyson, Rotational excitation with pointwise vibrational wavefunctions, *J. Chem. Phys.* 98 (1993) 9658–9668.
- A. Petrigiani, M. Berg, A. Wolf, I.I. Mizus, O.L. Polyansky, J. Tennyson, N.F. Zobov, M. Pavanello, L. Adamowicz, Visible intensities of the triatomic hydrogen ion from experiment and theory, *J. Chem. Phys.* 141 (2014) 241104, <http://dx.doi.org/10.1063/1.4904440>.
- A.J.C. Varandas, Energy switching approach to potential surfaces: An accurate single-valued function for the water molecule, *J. Chem. Phys.* 105 (1996) 3524–3531, <http://dx.doi.org/10.1063/1.473005>.
- O.L. Polyansky, A.A. Kyuberis, N.F. Zobov, J. Tennyson, S.N. Yurchenko, L. Lodi, ExoMol molecular line lists XXX: a complete high-accuracy line list for water, *Mon. Not. R. Astron. Soc.* 480 (2018) 2597–2608, <http://dx.doi.org/10.1093/mnras/sty1877>.
- I.I. Bubukina, N.F. Zobov, O.L. Polyansky, S.V. Shirin, S.N. Yurchenko, Optimized semiempirical potential energy surface for H<sub>2</sub><sup>16</sup>O up to 26000 cm<sup>-1</sup>, *Opt. Spectrosc.* 110 (2011) 186–193, <http://dx.doi.org/10.1134/S0030400X11020032>.
- S.N. Yurchenko, M. Carvajal, P. Jensen, F. Herregodts, T.R. Huet, Potential parameters of PH<sub>3</sub> obtained by simultaneous fitting of *ab initio* data and experimental vibrational band origins, *J. Chem. Phys.* 290 (2003) 59–67, [http://dx.doi.org/10.1016/S0301-0104\(03\)00098-3](http://dx.doi.org/10.1016/S0301-0104(03)00098-3).
- T. Odintsova, E. Fasci, L. Moretti, E.J. Zak, O.L. Polyansky, J. Tennyson, L. Gianfrani, A. Castrillo, Highly-accurate intensity factors of pure CO<sub>2</sub> lines near 2μm, *J. Chem. Phys.* 146 (2017) 244309, <http://dx.doi.org/10.1063/1.4989925>.
- G. Casa, R. Wehr, A. Castrillo, E. Fasci, L. Gianfrani, The line shape problem in the near-infrared spectrum of self-colliding CO<sub>2</sub> molecules: Experimental investigation and test of semiclassical models, *J. Chem. Phys.* 130 (2009) 184306, <http://dx.doi.org/10.1063/1.3125965>.
- A.J. Fleisher, H. Yi, A. Srivastava, O.L. Polyansky, N.F. Zobov, J.T. Hodges, Absolute <sup>13</sup>C/<sup>12</sup>C isotope amount ratio for Vienna PeeDee belemnite from infrared absorption spectroscopy, *Nat. Phys.* 17 (2021) 889–893, <http://dx.doi.org/10.1038/s41567-021-01226-y>.
- J.-K. Li, J. Wang, R.-H. Yin, Q. Huang, Y. Tan, C.-L. Hu, Y.R. Sun, O.L. Polyansky, N.F. Zobov, E.I. Lebedev, R. Stosch, J. Tennyson, G. Li, S.-M. Hu, Unprecedented accuracy in molecular line-intensity ratios from frequency-based measurement, *Sci. Adv.* (2025).